J Incl Phenom Macrocycl Chem (2014) 80:383–390
DOI 10.1007/s10847-014-0424-4

ORIGINAL ARTICLE

A fluorescent probe based on *N*-butylbenzene-1,2-diamine for Cu(II) and its imaging in living cells

Chunyan Zou · Lingzhi Gao · Tianyu Liu · Zhaochao Xu · Jingnan Cui

Received: 4 April 2014 / Accepted: 22 May 2014 / Published online: 6 June 2014

Abstract A fluorescent probe LZ-N with naphthalimide as fluorophore and *N*-butylbenzene-1,2-diamine as a new recognition moiety for copper ion was designed and synthesized. The probe LZ-N exhibits high selectivity for Cu^{2+} ion in aqueous media (CH_3CN:H_2O = 1:1) over all the other metal ions in our study, more than 20-fold fluorescence enhancement by coordinating with Cu^{2+}, and the maximum emission intensity independence in the range of pH 2.06–9.25. The results of ^{1}H-NMR titration, time-resolved fluorescence decay measurement, and computational optimization illuminate the mechanisms of Cu^{2+} and probe LZ-N. Confocal fluorescence images and cell viability values test show the high fluorescence enhancement of probe LZ-N for exogenous Cu^{2+} in living cells.

Keywords 1,8-Naphthalimide · *o*-*N*-Butylbenzene-1,2-diamine · Fluorescence · Probe · Copper ion · Live cells imaging

Introduction

Copper is the third most abundant essential transition metal ion in human body and plays a pivotal role in various physiological processes. Many proteins use it as an essential cofactor for electron transport, or as a catalyst in some oxidation–reduction reactions [1]. However, excess copper can catalyze the generation of reactive oxygen species (ROS) which can damage organisms. It has been reported that disorder of copper in cells can cause some neurodegenerative diseases such as Alzheimer's disease, Menkes and Wilson diseases [2–6]. Therefore, development of efficient detection methods for copper ion has received great concerns. Although several instrumental techniques have been developed to detect many heavy and transition metals [7–12], fluorescent probes are significant tools for sensing heavy and transition metals in biological bodies or environmental pollutions for its conveniences and high sensitivity [13–16]. Because Cu^{2+} is a fluorescent quencher by energy or electron transfer due to its nature of paramagnetism [17–19], a number of Cu^{2+} probes have been designed based on fluorescence quenching [18, 20–24]. For example, Ghosh [24] lately reported a benzothiazole-based receptor for Cu^{2+}, which is able to sense Cu^{2+} ion over a series of other metal ions by quenching of fluorescence to a greater extent (~78 %). The receptor has also been tested in aqueous CH_3CN (CH_3CN:H_2O = 4:1, v/v) and showed moderate binding of Cu^{2+} by 62 % quenching of emission which is not sensitive enough for the detection. Various fluorescence enhancement probes for Cu^{2+} have also been proposed so far [25–39]. However, some probes were only performed in pure organic solvents [33–37] which limited their use in biological samples. For example, Wei's group [33] recently reported a sugar-rhodamine fluorescent probe which exhibits a strong fluorescence signal to Cu^{2+} in acetonitrile media. However, the fluorescence was quickly quenched with the addition of water into acetonitrile medium, though this probe can dissolve in water-

Electronic supplementary material The online version of this article (doi:10.1007/s10847-014-0424-4) contains supplementary material, which is available to authorized users.

C. Zou · L. Gao · T. Liu · J. Cui (✉)
State Key Laboratory of Fine Chemicals, Dalian University of Technology, Dalian 116012, China
e-mail: jncui@dlut.edu.cn

Z. Xu
Dalian Institute of Chemical Physics, Chinese Academy of Sciences, Dalian 116023, China

Scheme 1 Synthesis of compound LZ-N

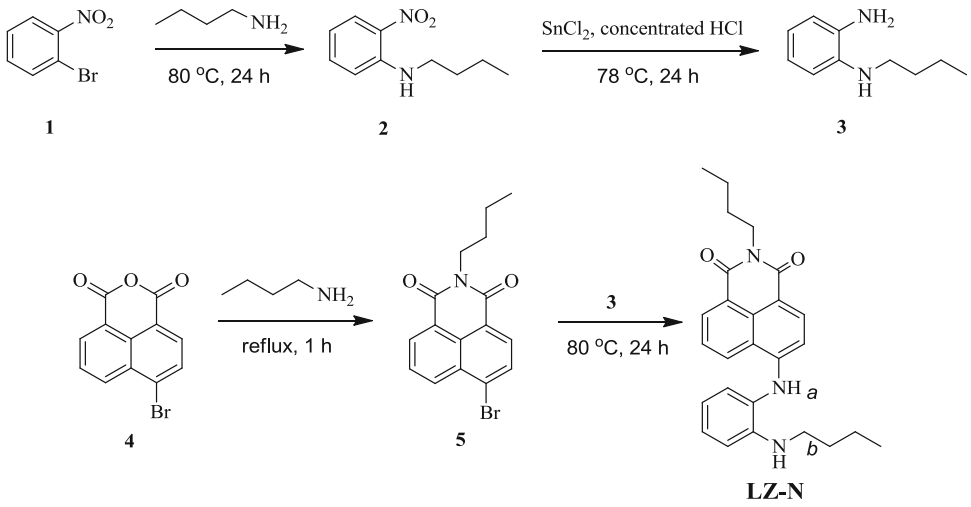

acetonitrile due to the inclusion of a sugar residue. The most probably reason was that the oxidation ability of Cu^{2+} was reduced significantly in water medium, which limited its biological applications. Besides, a few of these probes show poor selectivity to Cu^{2+} over other cations (Fe^{3+} and Zn^{2+}) [34, 35]. Hence, Cu^{2+} probes with high selectivity and readily applicable in bio-system are always needed.

1,8-Naphthalimide is a popular fluorophore due to its favorable properties, and we have reported some fluorescent probes with 1,8-naphthalimide as fluorophore [36–43], including some Cu^{2+} fluorescent probes [36–40]. In our previous study, two amine ligands had been introduced to 4 and 5 positions of 1,8-naphthalimide to form a tetra-dentate receptor, which appeared as a special cavity to bind with Cu^{2+} strongly [36–39] for nitrogen atoms bearing lone pair electrons to have certain coordination ability with metal ions. Among these, some fluorescent sensors are not highly selective [36, 37], which are interfered by other metal ions, such as Co^{2+}, Fe^{2+}, Ni^{2+}, Ag^{+}, and one is quenched by Cu^{2+} [38]. In this study, based on photoinduced electron transfer (PET) mechanism, we firstly introduced *o*-*N*-butylbenzene-1,2-diamine group into 4-position of 1,8-naphthalimide to obtain the fluorescent probe LZ-N (Scheme 1) via simple synthetic processes. For *o*-*N*-butylbenzene-1,2-diamine, two amino groups are fixed by benzene group, which can strengthen the recognition cavity. The amino cavity can coordinate with metal ions firmly preventing heavy metal to approach the fluorophore, and the benzene group is a π electron conjugate system which can improve the electron transfer between the *b*-position N of *o*-*N*-butylbenzene-1,2-diamine and the fluorophore, leading to more efficient PET effect. By binding Cu^{2+}, the probe is expected to recover the fluorescence of naphthalimide by blocking PET.

Experimental

Materials and instruments

All chemicals were analytical pure and used without further purification. All tested metal salts (almost perchlorate salts except $FeCl_3$ and $HgCl_2$) were purchased from Aldrich and Alfa Aesar. ^1H and ^{13}C-NMR spectra were recorded on a VARIAN INOVA-400 spectrometer (TMS as an internal standard). Mass spectrometry data were obtained with a HPLC-Q-TOF MS mass spectrometer. Fluorescence measurements were carried out on a JASCO FP-6500 fluorescence spectrophotometer. Absorption spectra were collected on a Hewlett-Packard HP-8453 UV–Vis spectrophotometer. The time-resolved fluorescence decays were measured using a Horiba Jobin–Yvon FluoroMax-4 spectrofluorometer.

As shown in Scheme 1, LZ-N was acquired from 4-bromo-*N*-butyl-1,8-naphthalimide and *N*-butylbenzene-1,2-diamine via substitution reaction, and the two intermediates were gotten with high yield from cheap and easy available starting materials. The structures of intermediate products and probe LZ-N were confirmed by ^1H and ^{13}C NMR, MS (Supporting Information, Fig. S 1–5).

Synthesis of 4-bromo-*N*-butyl-1,8-naphthalimide (**5**)

n-Butylamine (0.36 mL, 3.6 mmol) in ethanol (5.0 mL) was slowly dropped to a solution of 4-bromo-1,8-naphthalic anhydride **4** (1.0 g, 3.6 mmol) in 20 mL ethanol, and the solution was refluxed for 1.0 h. After cooling to room temperature, the yellowish precipitate was collected by filtration and then dried in a vacuum oven to give 5 (0.85 g, 71 %). M.P. 108.5–109.7 °C. ^1H NMR (400 MHz, $CDCl_3$, δ ppm) 8.63 (d, $J = 7.3$ Hz, 1H), 8.53 (d, $J = 8.5$ Hz, 1H), 8.38 (d, $J = 7.9$ Hz, 1H), 8.01 (d, $J = 7.9$ Hz, 1H), 7.82 (t,

1H), 4.26–4.07 (m, 2H), 1.71 (m, 2H), 1.52–1.37 (m, 2H), 0.98 (t, 3H).

Synthesis of *N*-butyl-2-nitroaniline (**2**)

n-Butylamine (14.4 mL, 14.4 mmol) in 4.0 mL DMSO was added to a solution of 2-bromonitrobenzene compound (0.80 g, 4.0 mmol) in 8.0 mL DMSO. Under N_2 gas, and the mixture was stirred at 80 °C for 24 h, then 30 mL water was added after cooling. The mixture was extracted with CH_2Cl_2 (40 mL × 3), and the combined CH_2Cl_2 layer was washed by brine, and dried over $MgSO_4$. The filtrate was concentrated to give **2** as yellow oil (0.73 g, 85 %).^{1}H NMR (400 MHz, $CDCl_3$, δ ppm) 8.16 (m, 1H), 8.05 (s, 1H), 7.42 (m, 1H), 6.85 (d, $J = 8.7$, 1H), 6.62 (d, $J = 8.7$ Hz, 1H), 6.62 (t, $J = 7.8$ Hz, 1H), 3.30 (t, $J = 7.1$ Hz, 2H), 1.77–1.68 (m, 2H), 1.54–1.43 (m, 2H), 0.99 (t, $J = 7.4$ Hz, 3H). TOF MS (ES+) *m/z* [$C_{10}H_{14}N_2O_2$] calcd. 194.1055, found: 194.9049.

Synthesis of *N*-butylbenzene-1,2-diamine (**3**)

$SnCl_2{\cdot}2H_2O$ (2.5 g, 11 mmol) in 4.0 mL concentrated HCl was slowly added to a mixture of compound **2** (0.71 g, 3.6 mmol) and 12 mL ethanol, and kept at 78 °C for 8 h. After being cooled to ambient temperature, the mixture was concentrated to remove ethanol, and the residue was treated with NaOH aqueous solution to adjust pH to neutral, and then extracted with CH_2Cl_2 (30 mL × 3). The combined organic layer was washed with dilute NaOH solution, and then dilute HCl solution (pH < 3) was added to the CH_2Cl_2 phase to adjust pH to acid. The aqueous phase was acquired to be adjusted pH to neutral again with dilute NaOH solution, and then the suspension was extracted with CH_2Cl_2 (30 mL × 3). The combined CH_2Cl_2 layer was dried over anhydrous $MgSO_4$. The filtrate was concentrated to give **3** as yellow waxy solid (0.60 g) which was used to the next step without further purification.

Synthesis of LZ-N

A mixture of compound **5** (1.1 g, 3.2 mmol), tris-(dibenzylideneacetone)dipalladium (0.030 g, 0.032 mmol), tri-*tert*-butylphosphonium tetrafluoroborate (0.028 g, 0.097 mmol), and anhydrous potassium tert-butylate (0.55 g, 4.9 mmol) in 10 mL dry toluene was added to the solution of compound **3** (0.60 g, crude) in 5.0 mL dry toluene under dry N_2 gas, and stirred at 80 °C for 24 h. Cooling to room temperature, some insoluble substance was filtrated off and the filtrate was concentrated. The crude product was purified by flash column chromatography (CH_2Cl_2) to obtain the compound LZ-N as an orange red solid (0.47 g, 35 %). M.P. 152.2–153.6 °C. ^{1}H NMR (400 MHz, CD_3SOCD_3, δ ppm) 8.97 (s, 1H), 8.89 (d, $J = 8.4$ Hz, 1H), 8.47 (d, $J = 7.3$ Hz, 1H), 8.18 (d, $J = 8.5$ Hz, 1H), 7.75 (t, $J = 7.8$ Hz, 1H), 7.20 (t, $J = 7.7$ Hz, 1H), 7.11 (d, $J = 7.6$ Hz, 1H), 6.78 (d, $J = 7.9$ Hz, 1H), 6.67 (t, $J = 7.4$ Hz, 1H), 6.37 (d, $J = 8.5$ Hz, 1H), 5.13 (s, 1H), 4.02 (t, $J = 7.3$ Hz, 2H), 3.08 (m, 2H), 1.64–1.54 (m, 2H), 1.50–1.42 (m, 2H), 1.38–1.22 (m, 4H), 0.92 (t, $J = 7.3$ Hz, 3H), 0.84 (t, $J = 7.3$ Hz, 3H).^{13}C NMR (100 MHz, $CDCl_3$, δ ppm) 164.69, 164.15, 147.91, 144.77, 134.03, 131.38, 129.96, 128.72, 127.45, 126.28, 125.39, 124.25, 123.47, 120.85, 117.39, 112.51, 111.85, 108.01, 43.55, 40.22, 31.59, 30.46, 20.60, 20.41, 14.07, 14.00. TOF MS (ES−) *m/z* [$C_{26}H_{29}N_3O_2$] calcd. 415.2260, found: 415.2246.

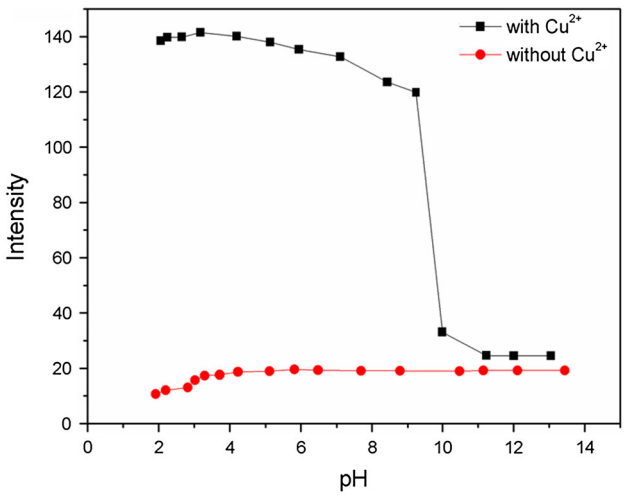

Fig. 1 Influence of pH on the fluorescence spectra ($\lambda_{ex} = 370$ nm) of LZ-N (10.0 μM) and LZ-N (10.0 μM) added Cu^{2+} (50 μM) in CH_3CN/H_2O solution (1:1, v:v). The pH was modulated by adding 1.0 M HCl or 1.0 M NaOH

Culture of MCF-7 cells and fluorescent imaging

MCF-7 (human breast carcinoma) was cultured in Dulbecco's modified Eagle's medium (DMEM, Invitrogen) supplemented with 10 % FBS (fetal bovine serum) in an atmosphere of 5 % CO_2 and 95 % air at 37 °C. The cells were seeded in 24-well flat-bottomed plates and then incubated under 5 % CO_2 for 24 h at 37 °C. The cells were incubated with probe LZ-N (5 μM) for 30 min and washed three times with PBS to remove the remaining probe. Then cells were treated with 25 μM $Cu(ClO_4)_2$ for another 30 min and washed with PBS for three times. The images of the MCF-7 cells were obtained by a fluorescence confocal microscopy (Olympus FV1000) with a 60× objective lens.

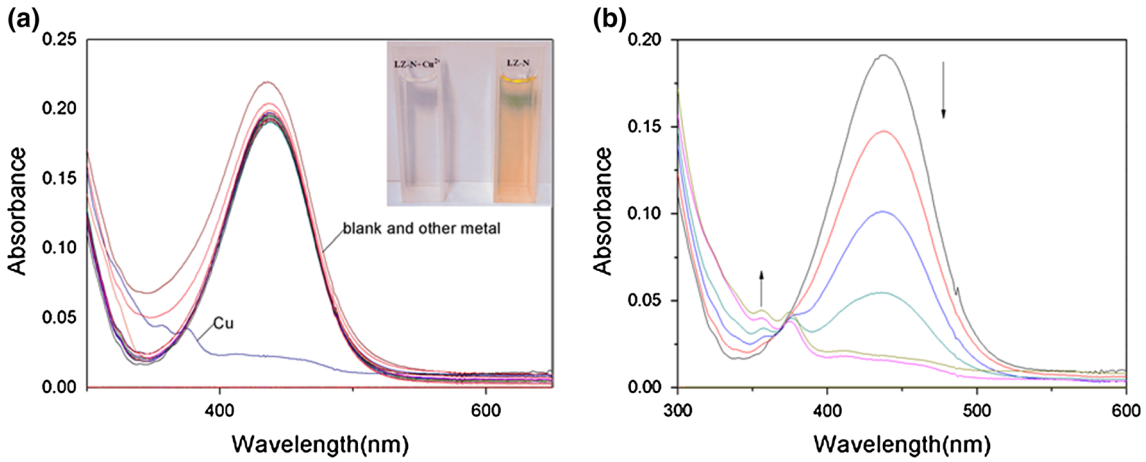

Fig. 2 **a** Absorbance spectra of LZ-N (10 μM) in CH_3CN/H_2O solution (1:1, v/v, 0.1 M HEPES buffer, pH 7.4) with different metal ions (50 μM, K^+, Na^+, Ag^+, Zn^{2+}, Cd^{2+}, Cu^{2+}, Hg^{2+}, Mg^{2+}, Ca^{2+}, Ba^{2+}, Co^{2+}, Al^{3+}, Cr^{3+}, Fe^{2+}, Fe^{3+}, Ni^{2+} and Pb^{2+}). **b** UV–Vis spectra of LZ-N (10 μM) in the presence of different amounts of Cu^{2+}. *Inset* Color change of the acetonitrile–water solutions of LZ-N (10 μM) on addition of Cu^{2+} (50 μM). (Color figure online)

Results and discussion

The pH titration was performed to investigate a suitable pH range for Cu^{2+} sensing in biological application. As shown in Fig. 1, the fluorescence intensities of metal-free LZ-N were very low at a very wide pH range due to PET. When the probe LZ-N was mixed with Cu^{2+}, the fluorescence recovered. The maximum emission intensity at 429 nm varied less than 14 % in the pH range of 2.06–9.25, though the fluorescence intensity changed a lot at pH values above 9.25. This indicates that the fluorescence "on–off" of probe LZ-N can be operated by Cu^{2+} addition in the pH range of 2.06–9.25, which is suitable for the physiological environment application.

To investigate the effects of probe LZ-N (10 μM) on metal ions, we tested the spectral response of LZ-N and LZ-N mixed with K^+, Na^+, Ag^+, Zn^{2+}, Cd^{2+}, Cu^{2+}, Hg^{2+}, Mg^{2+}, Ca^{2+}, Ba^{2+}, Co^{2+}, Al^{3+}, Cr^{3+}, Fe^{2+}, Fe^{3+}, Ni^{2+} and Pb^{2+}in the aqueous solution (CH_3CN :HEPES 1:1, v/v) (Fig. 2a). The maximum absorption peak at 438 nm is due to the absorption of naphthalimide part. With the increase of Cu^{2+}, the absorbance at 438 nm decreased sharply and a new peak at 357 nm was observed (Fig. 2b). The color of the solution changed from yellow to colorless which corresponds to a blue shift of about 70 nm. It results from the forming of Cu^{2+}–LZN complex which blocks the n–π transition between the *a*-position nitrogen atom in *o*-*N*-butylbenzene-1,2-diamine unit and fluorophore. Under the same conditions, LZ-N did not show any obvious color and spectra changes to other metal ions.

The fluorescence responses of LZ-N (10 μM) to metal ions in CH_3CN/H_2O solution were recorded in Fig. 3. LZ-N showed a very weak fluorescence in the absence of metal ions, and Cu^{2+} was the only metal ion to cause a remarkable blue emission (Fig. 3a). During sequential titration, a new emission band centered at 429 nm appeared, and a shoulder peak could be observed (Fig. 3b). To further study the interference by other metal ions, the competitive experiments were performed with other metal ions present mutually, including K^+, Na^+, Ag^+, Zn^{2+}, Cd^{2+}, Hg^{2+}, Mg^{2+}, Ca^{2+}, Ba^{2+}, Co^{2+}, Al^{3+}, Cr^{3+}, Fe^{2+}, Fe^{3+}, Ni^{2+} and Pb^{2+} (Fig. 4). The fluorescence enhancement induced by the mixtures of Cu^{2+} (50 μM) and most other metal ions (100 μM) was similar to that induced by Cu^{2+} alone. Increased fluorescence emission was only observed for mixtures of Cu^{2+} and Al^{3+} or Fe^{2+}, which means that Al^{3+} and Fe^{2+} may compete with Cu^{2+} to complex with LZN. These results indicates that most of the other metal ions do not affect the binding of compound LZ-N with Cu^{2+}, and Cu^{2+} is the only metal ion that can complex with compound LZ-N effectively (more than 20-fold enhancement at 429 nm), which is consistent with the absorption spectra results (Fig. 2). The detection limit of this probe for Cu^{2+} was calculated to be 3.97 μM based on $3 \times \delta_{blank}/k$ (where δ_{blank} is the standard deviation of the blank solution and k is the slope of the calibration plot). The results indicates that the probe LZ-N is capable of detecting Cu^{2+} on micromolar levels, which is lower than the limit for copper in drinking water set by the US Environmental Protection Agency (EPA) (roughly 20 μM), and is able to sufficiently sense the Cu^{2+} concentration in the blood system [18]. Based on the Job's plot analysis, it was showed probe LZN coordinated with Cu^{2+} in a ratio of 1:1 (Fig S6). It is preliminarily deduced that the fluorescence increase may come from the complex of one molecular probe LZN with one molecular copper ion via

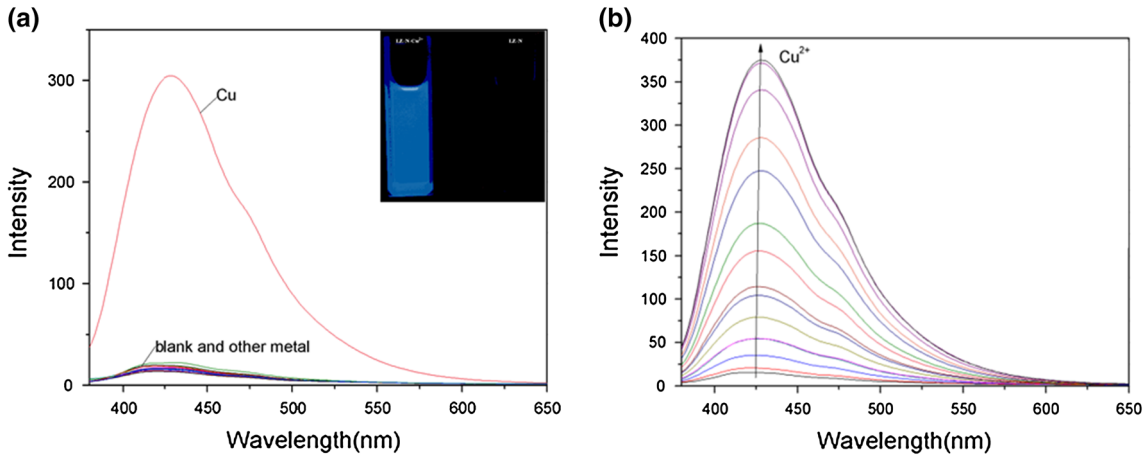

Fig. 3 **a** Fluorescence spectra of LZ-N (10 μM) in CH_3CN/H_2O solution (1:1, v/v, 0.1 M HEPES buffer, pH 7.4) with different metal ions (50 μM). *Inset* Fluorescence change of the CH_3CN/H_2O solutions of LZ-N (10 μM) on addition of Cu^{2+} (50 μM), $\lambda_{ex} = 370$ nm. **b** Fluorescence titration spectra of LZ-N (10 μM) in the presence of different amounts of Cu^{2+}

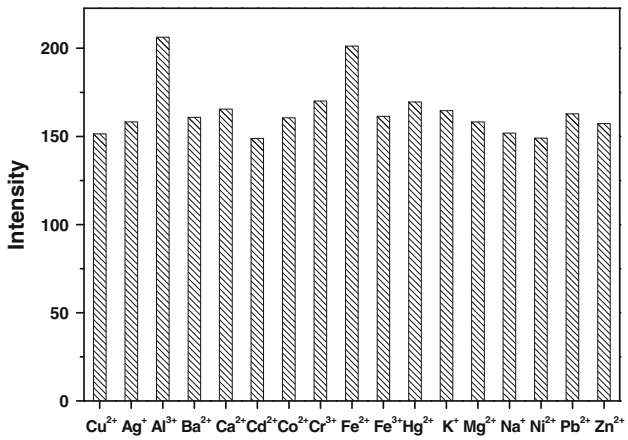

Fig. 4 Fluorescence intensity of LZ-N (10 μM) on the adding of Cu^{2+} (50 μM) in the absence and presence of different metal ions (100 μM) in CH_3CN/H_2O solution (1:1, v/v, 0.1 M HEPES buffer, pH 7.4)

two nitrogen atoms with the aid of benzene ring of the *o-N*-butylbenzene-1,2-diamine unit. Base on the titration data, the binding constant of LZN with Cu^{2+} in aqueous solution was calculated to be 3.88×10^5 M^{-1} [10].

It is well-known that one approach to prevent fluorescence quenching is to keep the heavy metal ions away from the fluorophore. To further understand the complexation between probe LZN and Cu^{2+}, ^1H NMR spectroscopy was used because Cu^{2+} can affect the resonance frequency of protons for its paramagnetic nature. The ^1H NMR spectra of probe LZN revealed that two amine protons (NH) signals at 8.97 ppm and 5.13 ppm completely disappeared upon the addition of 1 equiv. of Cu^{2+} (Fig. 5) and other peaks remained unchanged, indicating that Cu^{2+} binds to the two nitrogen atoms to avoid the fluorescence quenching of fluorophore.

The lifetime of the fluorescence decay is an important element for the mechanism. To get an insight into the complexation of LZN and Cu^{2+}, the fluorescence lifetime was measured in a concentration of 20 μM. The time-resolved fluorescence (TRF) behavior in the absence or presence of Cu^{2+} is shown in Fig. 6, and the exponential fit results are summarized in Table 1.

In the absence of Cu^{2+}, the fluorescence of LZN decayed biexponentially by 1.55 and 8.91 ns time constants, corresponding to two excitation states of free LZN, which could be verified by fluorescence spectra of LZ-N in various polarity solvents. For example, two emission spectra could be seen in low-polarity solvent (CCl_4) (Fig. S7). With the increasing of Cu^{2+}, the amount of slow decay component increased (from 21.2 to 55.7, 93.9, 94.2, and 94.2 % for 0.5, 1, 2, and 5 equiv of Cu^{2+}, respectively), while that of the fast decay component decreased accordingly. More importantly, when Cu^{2+} was added with more than 1.0 equiv., the time constant τ_2 of the lifetime decay component was mostly constant and the time constant τ_1 decreased to a constant value. This shows the fluorescence spectra come from two lifetime decay components, and the increase of τ_2 clearly indicates that the fluorescence increase derived from the slow decay component which may be LZN-Cu^{2+} complex.

The two nitrogen atoms in the *N*-butylbenzene-1,2-diamine play crucial roles for the photoelectron transfer, and as the *N*-butylbenzene-1,2-diamine is in the 4-position of the structure of LZ-N, there exists a *peri*-effect which could reduce the background fluorescence. After adding heavy metal ions, the N atoms of *o-N*-butylbenzene-1,2-diamine can coordinate Cu(II), which restrains the intramolecular charge transfer (ICT) to make a blue shift of the emission wavelength and blocks photo-induced electron

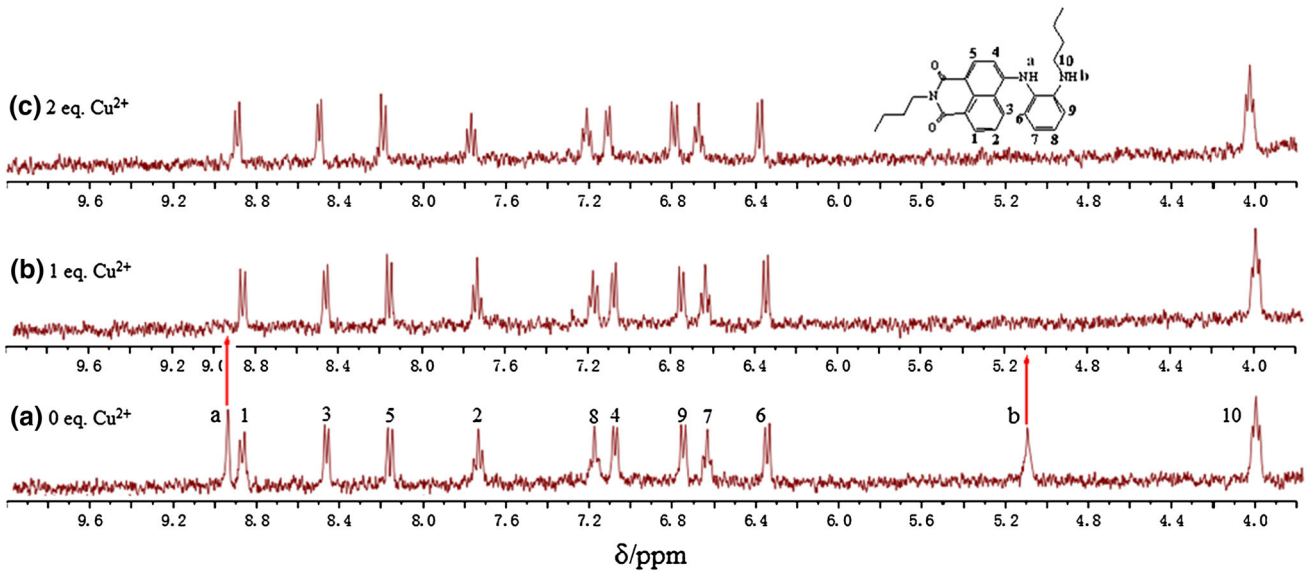

Fig. 5 ^{1}H-NMR (400 MHz) spectra of LZN in the presence of Cu^{2+} in DMSO-d_6

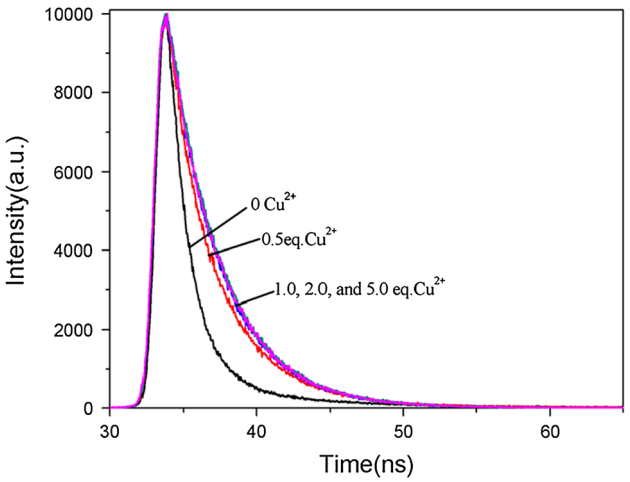

Fig. 6 Time-resolved fluorescence decay curves of LZ-N (20 μM) with an excitation at 376 nm and in the absence and presence of 0.5 equiv, 1.0 equiv, 2.0 equiv, and 5.0 equiv of Cu^{2+} ions

transfer (PET) to recover the fluorescence. Fig. S8 shows the optimized structures of LZ-N and the complex with Cu^{2+} using Dmol^3 package at the DFT PBE-DNP level. LZ-N and its Cu^{2+} complex present complete different frontier molecular orbitals, i.e. highest occupied molecular orbital (HOMO) and lowest unoccupied molecular orbital (LUMO). In the case of LZ-N, HOMO–LUMO excitation moves the electron density distribution from the *o*-*N*-butylbenzene-1,2-diamine moiety to the naphthalimide fluorophore, which leads to fluorescence quenching. In

Table 1 Fluorescence decay parameters of LZ-N with and without Cu^{2+}

Cu^{2+} (equiv.)	τ_1 (ns)	A_1 (%)	τ_2 (ns)	A_2 (%)	τ
0	1.55	78.8	8.91	21.2	3.11
0.5	2.34	44.3	5.12	55.7	3.89
1.0	0.47	6.12	4.03	93.9	3.81
2.0	0.22	5.81	4.05	94.2	3.82
5.0	0.25	5.78	4.03	94.2	3.81

contrast, in the case of LZ-N–Cu^{2+}, HOMO–LUMO excitation includes no such electron density shift which distributes mostly on the naphthalimide moiety. Therefore, the excited electrons would recess by emitting fluorescence.

As the compound could be used in neutral physiological condition, the fluorescence imaging of LZ-N before and after addition of Cu^{2+} was checked in MCF-7 cells (Fig. 7). The background fluorescence of LZ-N in cells was weak. With the addition of Cu^{2+}, the fluorescence intensity increased significantly. These results suggests that compound LZ-N can penetrate the cell membrane and might be used for detecting Cu^{2+} in living cells. The cytotoxicity of LN-Z was evaluated toward MCF-7 cells by a MTT assay (Fig. 8), and LN-Z was taken as concentrations from 0 to 10 μM. The results shows the cell viability remains at ~88 % after treatment with 10 μM of LN-Z for 48 h, which demonstrates low toxicity toward cultured cell.

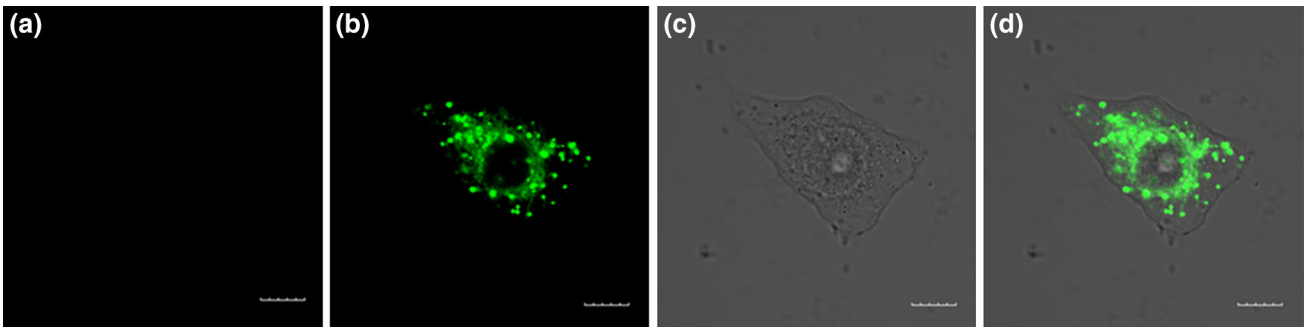

Fig. 7 Confocal fluorescence images in MCF-7 cells. **a** Cells incubated with 5 μM LZ-N in PBS buffer for 30 min; **b** cells were treated with 25 μM $Cu(ClO_4)_2$ for another 30 min and washed with PBS for three times; **c** bright field image of cells shown in panel; **d** merged image of **b** and **c**

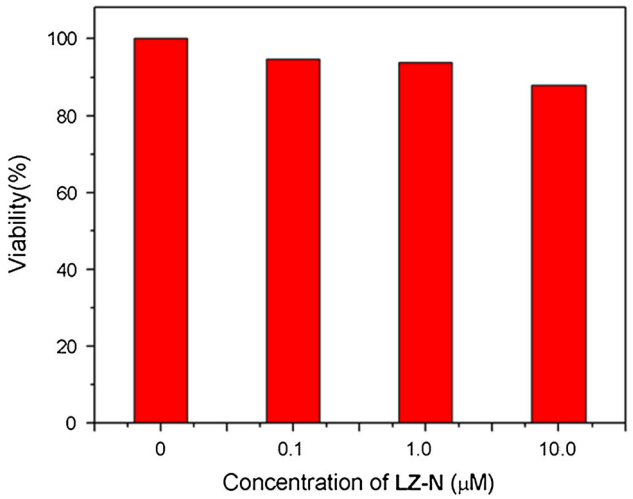

Fig. 8 Cell viability values (%) estimated by MTT test versus concentrations of LZ-N in MCF-7 cells

Conclusion

In summary, this study developed a new 1,8-naphthalimide-derived compound LZ-N for Cu^{2+} sensing by simple synthetic processes. Due to the unique structure of its *o-N*-butylbenzene-1,2-diamine recognition cavity, the probe can effectively complex with Cu^{2+} with high selectivity in aqueous solution (more than 20-fold fluorescence enhancement). It responds to Cu^{2+} with dual chromo- and fluorogenic-changes which realized "naked-eye" detection of Cu^{2+}. Moreover, the compound LZ-N is applicable to detect Cu^{2+} in living cells. This *o-N*-butylbenzene-1,2-diamine-based probe provides another simple identifying method for imaging Cu^{2+} in vitro and in vivo.

Acknowledgments We thank financial support from the National Key Project for Basic Research of China (2009CB724706).

References

1. Peter, C., Munoz, B., Sepulveda, F.J., Urrutia, J., Quiroz, M., Laza, S., De Ferrari, G.V., Aguayo, L.G., Opazo, C., De Ferrari, G.V., Aguayo, L.G., Opazo, C.: Biphasic effects of copper on neurotransmission in rat hippocampal neurons. J. Neurochem. **119**, 78–88 (2011)
2. Hung, Y.H., Bush, A.I., Cherny, R.A.: Copper in the brain and Alzheimer's disease. J. Biol. Inorg. Chem. **15**, 61–76 (2010)
3. Waggoner, D.J., Bartnikas, T.B., Gitlin, J.D.: The role of copper in neurodegenerative disease. Neurobiol. Disease **6**, 221–230 (1999)
4. Vulpe, C., Levinson, B., Whitney, S., Packman, S., Gitschier, J.: Isolation of a candidate gene for Menkes disease and evidence that it encodes a copper-transporting ATPase. Nat. Genet. **3**, 7–13 (1993)
5. Que, E.L., New, E.J., Chang, C.J.: A cell-permeable gadolinium contrast agent for magnetic resonance imaging of copper in a Menkes disease model. Chem. Sci. **3**, 1829–1834 (2012)
6. Vonk, W.I.M., de Bie, P., Wichers, C.G.K., van den Berghe, P.V.E., van der Plaats, R., Berger, R., Wijmenga, C., Klomp, L.W.J., van de Sluis, B.: The copper-transporting capacity of ATP7A mutants associated with Menkes disease is ameliorated by COMMD1 as a result of improved protein expression. Cell. Mol. Life Sci. **69**, 149–163 (2012)
7. Zhang, J.F., Zhou, Y., Yoon, J., Kim, J.S.: Recent progress in fluorescent and colorimetric probes for detection of precious metal ions (silver, gold and platinum ions). Chem. Soc. Rev. **40**, 3416–3429 (2011)
8. Cao, H.Y., Shi, W.B., Xie, J.X., Huang, Y.M.: Highly sensitive and selective fluorescent assay for quantitative detection of divalent copper ion in environmental water samples. Anal. Methods **3**, 2102–2107 (2011)
9. Shao, N., Jin, J.Y., Wang, H., Zhang, Y., Yang, R.H., Chan, W.H.: Tunable photochromism of spirobenzopyran via selective metal ion coordination: an efficient visual and ratioing fluorescent probe for divalent copper ion. Anal. Chem. **80**, 3466–3475 (2008)
10. Zhao, Y., Zhang, X.B., Han, Z.X., Qiao, L., Li, C.Y., Jian, L.X., Shen, G.L., Yu, R.Q.: Highly sensitive and selective colorimetric and Off-On fluorescent chemosensor for Cu^{2+} in aqueous solution and living cells. Anal. Chem. **81**, 7022–7030 (2009)
11. Aksunera, N., Henden, E., Yilmaz, I., Cukurovali, A.: A highly sensitive and selective fluorescent sensor for the determination of copper (II) based on a schiff base. Dyes Pigments **83**, 211–217 (2009)

12. Huo, F.J., Yin, C.X., Yang, Y.T., Su, J., Chao, J.B., Liu, D.S.: Ultraviolet-visible light (UV−Vis)-reversible but fluorescence-irreversible chemosensor for copper in water and its application in living cells. Anal. Chem. **84**, 2219–2223 (2012)
13. Liu, J.W., Lu, Y.: A DNAzyme catalytic beacon sensor for paramagnetic Cu^{2+} ions in aqueous solution with high sensitivity and selectivity. J. Am. Chem. Soc. **129**, 9838–9839 (2007)
14. Son, H., Kang, G., Jung, J.H.: A thin-layer chromatography plate prepared from BODIPY-based receptor immobilized SiO_2 nanoparticles as a portable chemosensor for Pb^{2+}. Analyst **137**, 163–169 (2012)
15. Cheng, T.Y., Wang, T., Zhu, W.P., Chen, X.L., Yang, Y.J., Xu, Y.F., Qian, X.H.: Red-emission fluorescent probe sensing cadmium and pyrophosphate selectively in aqueous solution. Org. Lett. **13**, 3656–3659 (2011)
16. Liu, X.J., Zong, C.H., Lu, L.H.: Fluorescent silver nanoclusters for user-friendly detection of Cu^{2+} on a paper platform. Analyst **137**, 2406–2414 (2012)
17. de Silva, A.P., Gunaratne, H.Q.N., Gunnlaugsson, T.H., Allen, J.M., McCoy, C.P., Rademacher, J.T., Rice, T.E.C.: Signaling recognition vents with fluorescent sensors and switches. Chem. Rev. **97**, 1515–1566 (1997)
18. Jung, H.S., Kwon, P.S., Lee, J.W., Kim, J.I., Hong, C.S., Kim, J.W., Yan, S.H., Lee, J.Y., Lee, J.H., Joo, T.H., Kim, J.S.: Coumarin-derived Cu^{2+}-selective fluorescence sensor: synthesis, mechanisms, and applications in living cells. J. Am. Chem. Soc. **131**, 2008–2012 (2009)
19. Royzen, M., Dai, Z.H., Canary, J.W.: Ratiometric displacement approach to Cu (II) sensing by fluorescence. J. Am. Chem. Soc. **127**, 1612–1613 (2005)
20. Mashraqui, S.H., Khan, T., Chandiramani, M., Betkar, R., Poonia, K.: Anthracene-tethered aminomethyl oxadiazole chemosensor: a probe offering selective chromo- and fluorogenic signaling for targeting Cu(II). J. Incl. Phenom. Macrocycl. Chem. **67**, 361–367 (2010)
21. Ando, H., Ichihashi, Y., Tawa, K., Tanaka, M.: XAFS study of the complex of an acetylacetonate-based ligand and copper ion. J. Incl. Phenom. Macrocycl. Chem. **71**, 293–296 (2011)
22. Guo, Q.N., Zhong, C., Lu, Y.G., Shi, C., Li, Z.Y.: Dipyrrolylquinoxaline-bridged hydrazones: a new class of chemosensors for copper(II). J. Incl. Phenom. Macrocycl. Chem. **72**, 79–88 (2012)
23. Liu, Z.C., Yang, Z.Y., Li, T.R., Wang, B.D., Li, Y., Qin, D.D., Wang, M.F., Yan, M.H.: An effective Cu(II) quenching fluorescence sensor in aqueous solution and 1D chain coordination polymer framework. Dalton Trans. **40**, 9370–9373 (2011)
24. Ghosh, K., Kar, D.: Anthraquinone coupled benzothiazole-based receptor for selective sensing of Cu^{2+}. J. Incl. Phenom. Macrocycl. Chem. **77**, 67–74 (2013)
25. Kim, S.H., Kim, J.S., Park, S.M., Chang, S.K.: Hg^{2+}-selective OFF–ON and Cu^{2+}-selective ON–OFF type fluoroionophore based upon cyclam. Org. Lett. **8**, 371–374 (2006)
26. Algi, M.P., Öztaş, Z., Algi, F.: Triple channel responsive Cu^{2+} probe. Chem. Commun. **48**, 10219–10221 (2012)
27. Zhang, J., Yu, C.W., Qian, S.Y., Lu, G., Chen, J.L.: A selective fluorescent chemosensor with 1, 2,4-triazole as subunit for Cu (II) and its application in imaging Cu (II) in living cells. Dyes Pigments **92**, 1370–1375 (2012)
28. Cui, S.Q., Pu, S.Z., Liu, W.J.: Synthesis and photochromic properties of a multiple responsive diarylethene and its selective binding affinity for copper (II) ion. Dyes Pigments **91**, 435–441 (2011)
29. Jo, J.Y., Lee, H.Y., Liu, W.J., Olasz, A., Chen, C.H., Lee, D.W.: Reactivity-based detection of copper (II) ion in water: oxidative cyclization of azoaromatics as fluorescence turn-on signaling mechanism. J. Am. Chem. Soc. **134**, 16000–16007 (2012)
30. Zhou, Y., Wang, F., Kim, Y., Kim, S.J., Yoon, J.: Cu^{2+}-selective ratiometric and "Off-On" sensor based on the rhodamine derivative bearing pyrene group. Org. Lett. **11**, 4442–4445 (2009)
31. Zhao, C.C., Feng, P., Cao, J., Wang, X.Z., Yang, Y., Zhang, Y.L., Zhang, J.X., Zhang, Y.F.: Borondipyrromethene-derived Cu^{2+} sensing chemodosimeter for fast and selective detection. Org. Biomol. Chem. **10**, 3104–3109 (2012)
32. Yuan, L., Lin, W.Y., Chen, B., Xie, Y.N.: Development of FRET-based ratiometric fluorescent Cu^{2+} chemodosimeters and the applications for living cell imaging. Org. Lett. **14**, 432–435 (2012)
33. Yin, J.X., Ma, X., Wei, G.H., Wei, D.B., Du, Y.G.: A highly selective and sensitive sugar–rhodamine "turn-on" fluorescent sensor for divalent copper ion detection in acetonitrile. Sens. Actuators B Chem. **177**, 213–217 (2013)
34. Martínez, R., Zapata, F., Caballero, A., Espinosa, A., Tárraga, A., Pedro, M.: 2-Aza-1,3-butadiene derivatives featuring an anthracene or pyrene unit: highly selective colorimetric and fluorescent signaling of Cu2+ cation. Org. Lett. **8**, 3235–3238 (2006)
35. Wen ZC, Yang R, He H, Jiang YB: A highly selective charge transfer fluoroionophore for Cu2+. Chem. Commun. 106–108 (2006)
36. Xu, Z.C., Qian, X.H., Cui, J.N.: Colorimetric and ratiometric fuorescent chemosensor with a large red-shift in emission: Cu(II)-only sensing by deprotonation of secondary amines as receptor conjugated to naphthalimide fuorophore. Org. Lett. **7**, 3029–3032 (2005)
37. Xu, Z.C., Qian, X.H., Cui, J.N., Cui, D.W.: Ratiometric and selective fluorescent sensor for Cu^{II} based on internal charge transfer (ICT). Org. Lett. **7**, 889–892 (2005)
38. Chen, X.F., Wang, J.Y., Cui, J.N., Xu, Z.C., Peng, X.J.: A ratiometric and exclusively selective Cu^{II} fluorescent probe based on internal charge transfer (ICT). Tetrahedron **67**, 4869–4873 (2011)
39. Xu, Z.C., Baek, K.H., Kim, H.N., Cui, J.N., Qian, X.H., Spring, D.R., Shin, I., Yoon, J.Y.: Zn^{2+} -triggered amide tautomerization produces a highly Zn^{2+}-selective, cell-permeable, and ratiometric fluorescent sensor. J. Am. Chem. Soc. **132**, 601–610 (2010)
40. Xu, Z.C., Pan, J., Spring, D.R., Cui, J.N., Yoon, J.Y.: Ratiometric fluorescent and colorimetric sensors for Cu^{2+} based on 4,5-disubstituted-1,8-naphthalimide and sensing cyanide via Cu^{2+} displacement approach. Tetrahedron **66**, 1678–1683 (2010)
41. Lu, C.L., Xu, Z.C., Cui, J.N., Zhang, R., Qian, X.H.: Ratiometric and highly selective fluorescent sensor for cadmium under physiological pH range: a new strategy to discriminate cadmium from zinc. J. Org. Chem. **72**, 3554–3557 (2007)
42. Wang, M., Xu, Z.C., Wang, X., Cui, J.N.: A fluorescent and colorimetric chemosensor for nitric oxide based on 1,8-naphthalimide. Dyes Pigments **9**, 333–337 (2013)
43. Liu, T.Y., Xu, Z.C., Spring, D.R., Cui, J.N.: A lysosome-targetable fluorescent probe for imaging hydrogen sulfide in living cells. Org. Lett. **15**, 2310–2313 (2013)